

Inferences on the upper crustal structure of Southern Apennines (Italy) from seismic refraction investigations and subsurface data

Luigi Improta^{a,*}, Giovanni Iannaccone^b, Paolo Capuano^b, Aldo Zollo^a,
P. Scandone^c

^a *Dipartimento di Scienze Fisiche, Università di Napoli 'Federico II', Napoli, Italy*

^b *Osservatorio Vesuviano, Napoli, Italy*

^c *Dipartimento di Scienze della Terra, Università degli Studi di Pisa, Pisa, Italy*

Received 26 April 1999; accepted for publication 21 October 1999

Abstract

This paper presents an interpretation of crustal seismic refraction data from the northern sector of the Southern Apennines thrust belt, a region that in historical times experienced large destructive earthquakes. The data were acquired in 1992 along a seismic line 75 km long and parallel to the Apenninic chain, in order to determine a detailed 2-D P-wave velocity model of the upper crust in an area that had not been deeply investigated by geophysical methods previously. We have used a 2-D ray tracing technique based on asymptotic ray theory to model travel times of first and reflected P-wave arrivals. Synthetic seismograms have been produced by finite difference simulations in order to check the reliability of the velocity model inferred by ray-tracing modelling. The interpretation of the velocity model is constrained by stratigraphic and sonic velocity logs from wells for oil exploration located close to the seismic line. Gravity data modelling allows to check the velocity model and to extend the structural interpretation in 3-D. In the shallow crust, up to a depth of 3–4 km, strong lateral variations of the modelled velocities are produced by the overlapping of thrust sheets formed by: (1) Cenozoic flyschoid cover and basal successions that underlie the seismic profile with P-wave velocities in the 2.8–4.1 km/s range and thicknesses varying between 0.5 and 4.5 km; (2) Mesozoic basal sequences with a velocity of 4.8 km/s and a depth of 1.5–2.1 km in the northern part of the profile; (3) Mesozoic limestones of the Western Carbonate Platform with a velocity of 6.0 km/s and a depth of 0.1–0.8 km in the southern part of the profile. At a greater depth, the model becomes more homogeneous. A continuous seismic interface 3.0–4.5 km deep with a velocity of 6.0 km/s is interpreted as the top of the Meso-Cenozoic Carbonate Multilayer of the Apulia Platform, characterized by an increase in seismic velocity from 6.2 to 6.6 km/s at depths of 6–7 km. A lower P-wave velocity (about 5.0 km/s) is hypothesized at depths ranging between 9.5 and 11 km. As inferred by commercial seismic lines and data from two deep wells located in the Apulia foreland and Bradano foredeep, this low-velocity layer can be related to Permo-Triassic clastic deposits drilled at the bottom of the Apulia Platform. Seismic data do not allow us to identify possible deeper seismic interfaces that could correspond to the top of the Paleozoic crystalline basement; this is probably due to the low-velocity layer at the bottom of the Carbonate Multilayer that reflects and attenuates a great part of the seismic energy. The joint interpretation of seismic refraction and well data, in accordance with gravity data, provides the first detailed P-wave velocity model of the upper crust of the northern sector of the Southern Apennines, which differs considerably from previous 1-D velocity models used

* Corresponding author. Tel.: +39-81-7253307; fax: +39-81-7253452.

E-mail address: gigi@na.infn.it (L. Improta)

to study the seismicity of the region, and reveals new information about the structure of the thrust belt. © 2000 Elsevier Science B.V. All rights reserved.

Keywords: crustal structure; Italy; seismic refraction; Southern Apennines

1. Introduction

The Southern Apennines is a Neogene thrust belt resulting from the deformation of the Apulian continental margin. As inferred by earthquake fault plane solutions (Anderson and Jackson, 1987) and present-day stress data (Amato and Montone, 1997), this region is subject to a widespread crustal extension perpendicular to the chain. The Southern Apennines are characterized by a narrow seismic belt, NW–SE-striking and 30–50 km wide approximately following the axis of the chain.

The northern sector of Southern Apennines, the Sannio region, is among the most active seismic regions in Italy. In the last three centuries, it has been struck by four large destructive earthquakes occurring in 1688 ($I_0 = \text{XI MCS}$), 1702 ($I_0 = \text{X}$), 1732 ($I_0 = \text{X}$) and 1805 ($I_0 = \text{X}$). Since 1805, a period of seismic quiescence, broken off only by three moderate-magnitude events ($M_s = 5.7$, $M_s = 6.1$, $M_s = 5.4$), occurring on the 22nd August 1962, has followed. At present, the seismicity is characterized by low-energy earthquakes frequently clustered in swarms occurring at the borders of primary faults, which caused the most energetic earthquakes. The long quiescence following the 1805 event makes the Sannio region one of the most likely candidates for future large destructive events in Italy.

In 1992, a seismic survey was carried out in this area of Southern Apennines with two main goals: (1) to perform a local seismic response study in Benevento, the main town of the region (Iannaccone et al., 1995; Marcellini et al., 1995a,b); (2) to provide a seismic velocity model of the Sannio region. In fact, the availability of a reliable velocity model and the knowledge of the crustal structure are essential elements to compute accurate hypocentral locations and fault plane solutions in order to understand the relation

between tectonics and the present-time, low-magnitude seismicity of this region. A description of the seismic survey and a preliminary analysis of data was reported by Iannaccone et al. (1998).

In this paper, we present a detailed P-wave velocity and structural model of the upper crust of a sector of the Southern Apennines that includes the Sannio region and the northern end of the Irpinia region (Fig. 1), where, in 1980, an $M_s = 6.9$ normal faulting earthquake occurred (Bernard and Zollo, 1989). The model is obtained by a joint interpretation of five seismic refraction profiles recorded during the 1992 survey along a main line 75 km long, well data and commercial seismic lines. Moreover, the reliability of the inferred model is ensured by a finite difference waveform modelling and gravity data modelling.

2. Geological and geophysical setting

The Southern Apennines is an east-verging accretionary wedge developed in Neogene times above a west-dipping subduction of the Apulian–Ionian lithosphere (Doglioni et al., 1996). The arc-shaped chain is associated with a back-arc extensional basin, the Tyrrhenian basin. From Late Tortonian to Quaternary, extension in the Tyrrhenian basin and thrust propagation in the mountain belt coexisted and rapidly migrated eastwards. Migration of the back-arc basin/thrust belt/foredeep system was controlled by the eastward retreat of the sinking foreland lithosphere (Malinverno and Ryan, 1986; Patacca and Scandone, 1989).

The geological structure of the Sannio and Irpinia regions is not clear at present because of the complexity of the paleogeographic domains involved in the mountain chain building. Moreover, compression did not propagate cylindrically and was characterized by the development of

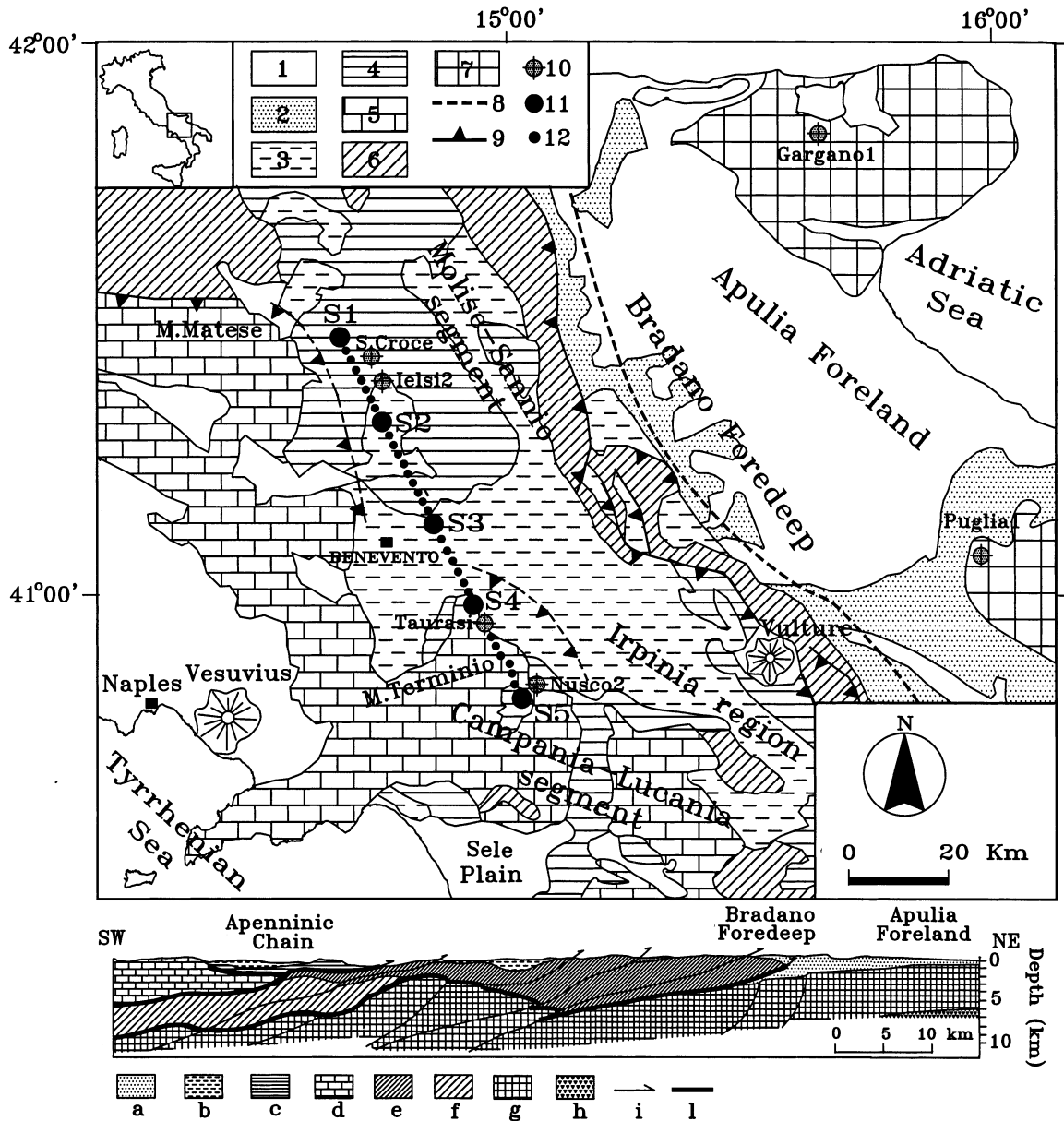


Fig. 1. Simplified geological sketch of the Southern Apennines. 1 — Middle–Upper Pleistocene and Holocene deposits; 2 — Upper Pliocene–Lower Pleistocene deposits; 3 — Upper Tortonian to Upper Pliocene thrust-sheets-top deposits; 4 — Sannio and Sicilide nappes (Paleogene–Lower Miocene); 5 — Western Carbonate Platform (Mesozoic–Tertiary) and unconformable Upper Miocene siliciclastic flysch deposits of the related marginal areas; 6 — Lagonegro and Molise Basin sequences (Mesozoic–Tertiary); 7 — Apulia Carbonate Platform (Mesozoic–Tertiary); 8 — buried frontal ramp of the Apennine thrust sheets; 9 — out of sequence thrust; 10 — well; 11 — shot point; 12 — seismic station. Schematic geological cross-section of the northern sector of the Southern Apennines. (a) Plio-Pleistocene deposits of the Bradano foredeep; (b) Late Tortonian to Upper Pliocene thrust-sheets-top deposits; (c) Sannio nappe (Paleogene–Lower Miocene); (d) Western Carbonate Platform (Mesozoic–Tertiary) and unconformable Upper Miocene flysch deposits of the related marginal areas; (e) Lagonegro and Molise Basin upper sequence (Cenozoic); (f) Lagonegro and Molise Basin lower sequence (Mesozoic); (g) Apulia Carbonate Platform (Mesozoic–Tertiary); (h) Verrucano formation (Permian–Lower Triassic); (i) thrust planes; (l) boundary of the main nappes.

out-of-sequence thrusts, which further complicate the structure of the Apenninic accretionary wedge (Roure et al., 1991).

Regional synthesis of the upper crustal structure of a large portion of Southern Italy was realized by jointly interpreting geological studies and proprietary well and seismic reflection data for oil exploration (Mostardini and Merlini, 1986; Roure et al., 1991). In particular, Mostardini and Merlini (1986) proposed a structural model of the Southern Apennines consisting of 15 geological cross-sections cutting the Apenninic chain in NE–SW direction from the Tyrrhenian to the Adriatic sea. In this paper, we will compare our model, obtained by interpreting seismic refraction, well and gravity data, with four of these sections, which have been crossed by the seismic refraction line.

In the investigated area, the accretionary wedge consists of a pile of nappes forming a duplex system orogenically transported over the flexured south-western margin of the Apulia foreland (Fig. 1) (Patacca and Scandone, 1989). It incorporates Meso–Cenozoic sedimentary domains including basins and shelves of the Apulia continental margin. The tectonic units underlying the roof-thrust are represented by Meso–Cenozoic carbonates of the Apulia Carbonate Platform, disconformably overlain by Upper Messinian carbonates and evaporites and Pliocene terrigenous marine deposits; they are involved in the folds and thrusts of a buried thrust belt (Fig. 1) detected by commercial seismic profiles and explored by several wells (Mostardini and Merlini, 1986).

Above the roof-thrust, three groups of nappes can be distinguished: (1) nappes derived from the Lagonegro–Molise Basin (originally located between the Apulia Platform and the Western Carbonate Platform); (2) nappes derived from the Western Carbonate Platform and from related marginal areas (including unconformable Upper Miocene flysch deposits); (3) nappes derived from more internal basins (Sicilide and Sannio nappes) deformed before the opening of the Tyrrhenian basin and now forming the highest units of the duplex system (for a review, see Marsella et al., 1995).

Piggyback basins, developed on top of the advancing thrust sheets from Messinian to Late

Pliocene–Pleistocene times, have been progressively filled in by different sedimentary sequences, at present widely outcropping in the study area. Upper Pliocene–Lower Pleistocene out-of-sequence thrusts are responsible for the present-day arrangement of the Southern Apennines into the Molise–Sannio and Campania–Lucania arcuate segments, characterized by a NNW–SSE- and WNW–ESE-trending of the compressive fronts, respectively (Fig. 1). During the Middle Pleistocene, the Southern Apenninic wedge has been uplifted and involved in an extensional tectonic event with a NE–SW direction cross-cutting the contractional structures. This stress regime is responsible for the historical and present-day seismic activity (Anderson and Jackson, 1987).

The chain was not investigated in detail by geophysical methods. Prior to our study, the only seismic data available were two scanty seismic refraction/wide angle reflection profiles conducted in the 1970s, as part of the DSS (Deep Seismic Soundings) program carried out within the frame of the European Seismological Commission (Italian Explosion Seismology Group, 1982). Data interpretation provides some indications about the depth of the Moho boundary in the transitional area between the Southern and Central Apennines but does not allow definition of a detailed velocity model of the upper crust.

A 3-D P-wave velocity model of the upper crust beneath the Sannio area has recently been presented by Chiarabba and Amato (1997) as result of a tomographic study, performed using the background seismicity recorded in 1991 and 1992 by a local seismic array. The tomographic results show a pattern of strong velocity anomalies in the shallow crust (upper 6 km of depth) that has been related to lithological heterogeneities between limestones of carbonate platforms (high velocities) and basal sequences (low velocities), which characterize the tectonic setting of the Southern Apennines. At a greater depth (9 km), the velocity model becomes more homogeneous and presents two NW-trending high-velocity zones ($V_p \sim 6.3$ km/s), which have been interpreted as an upthrust of lower-crust rocks; this structural interpretation implies the involvement of lower crustal

wedges in the compressional tectonics during the Southern Apennines orogenesis.

Regional scale studies, about the lithospheric structure beneath the Tyrrhenian basin, Apennines and Apulia foreland, analyse gravity (Corrado and Rapolla, 1981) and magnetic (Fedi and Rapolla, 1990) field in Central and Southern Italy, trying a first attempt to a large-scale crustal model.

3. Well data interpretation

Stratigraphic and sonic velocity logs from four wells located close to the seismic refraction profile have been interpreted in order to constrain the shallow part of the velocity and structural models up to a depth of about 3.0 km.

Stratigraphic logs from Ielsi 2 (765 m a.s.l.; total depth 3195 m) and S. Croce wells (840 m a.s.l.; T.D. 2757 m) (Fig. 2), located a few kilometres east of the northern part of the refraction line (Fig. 1), show the tectonic superposition of the Sannio nappe, mainly consisting of plastically deformed varicoloured clays and Paleogene–Lower Miocene limestones and coarse-clastic lime resediments, over the Molise nappe (Patacca and Scandone, 1992). The latter is represented by Mesozoic–Tertiary basinal deposits locally forming quite complex imbricated structures. The Jurassic–Lower Cretaceous portion of the Molise sequence is made up of dolomitized breccias and calciturbidites (Patacca and Scandone, 1992) well recognizable in commercial seismic lines due to their reflectivity. These high-velocity deposits, cropping out north of Matese Mountain (Fig. 1), have been drilled in the Sannio region by several wells.

Stratigraphic and sonic logs from Taurasi well (340 m a.s.l.; T.D. 3476 m) (Fig. 2), located on the seismic profile 2 km south of shot S4 (Fig. 1), have been helpful in model seismic refraction data and in providing a structural interpretation of the resulting velocity model because the drilling explored the top of the Apulia Carbonate Platform. Cretaceous limestones, with a seismic velocity of 6.0 km/s, stratigraphically covered by Messinian anhydrites several tens of metres thick, have been penetrated at about 3.0 km of depth.

The evaporitic layer is tectonically overlain by a pile of several thrust sheets. The highest, 1.1 km thick, consists of Upper Tortonian flysch deposits with a seismic velocity in the 3.3–3.5 km/s range. The others are formed by chaotic varicoloured clays and Late Tortonian–Upper Messinian sandstones and limestones with repeated evaporitic layers. As inferred by sonic logs, low-velocity (3.4–3.6 km/s) and high-velocity (4.1–5.2 km/s) intervals succeed from 0.8 km down to 3.0 km of depth, in correspondence with varicoloured clays and limestones with evaporitic layers, respectively.

A different structural framework has been observed in Nusco 2 well (700 m a.s.l. and T.D. 1400) located 2 km east of shot S5 (Fig. 1). Mesozoic limestones of the Western Carbonate Platform (Fig. 2) were found between 0.6 km depth down to the bottom of the well. The latter crops out several kilometres east of the seismic line in the Terminio Mountain (Fig. 1). The Mesozoic limestones are unconformably overlain by Upper Miocene flysch deposits, which are tectonically covered, in turn, by the Sicilide and Sannio nappes; these low-velocity deposits exceed 1 km in thickness.

Sonic and stratigraphic logs from Puglia 1 (544 m a.s.l.; T.D. 7070 m) and Gargano 1 (73 m a.s.l.; T.D. 4224 m) wells, located about 100 km east of the seismic line in the Apulia foreland (Fig. 1), have been interpreted in order to understand the reliability and the structural meaning of two deep (about 6 and 11 km depth) seismic discontinuities detected by refraction data and probably related to the Apulia Carbonate Multilayer. In fact, these are the only two deep wells of Southern Italy that have crossed the whole Apulia Carbonate Platform, drilling at its bottom, sedimentary Paleozoic strata.

Puglia 1 well penetrates: (1) Cretaceous–Liassic limestones, dolomit limestones and dolomites from 0 m to 3535 m, (2) dolomites of uncertain age (scarce or no recovery of cuttings) from 3535 to 5000 m, (3) Triassic dolomites and anhydrites of the Burano formation from 5000 to 6112 m and finally (4) Lower Triassic–Permian siliciclastic deposits referable to the Verrucano formation from 6112 to the final depth (7070 m) (Fig. 2). The sonic log displays seismic velocities in the 6.0–

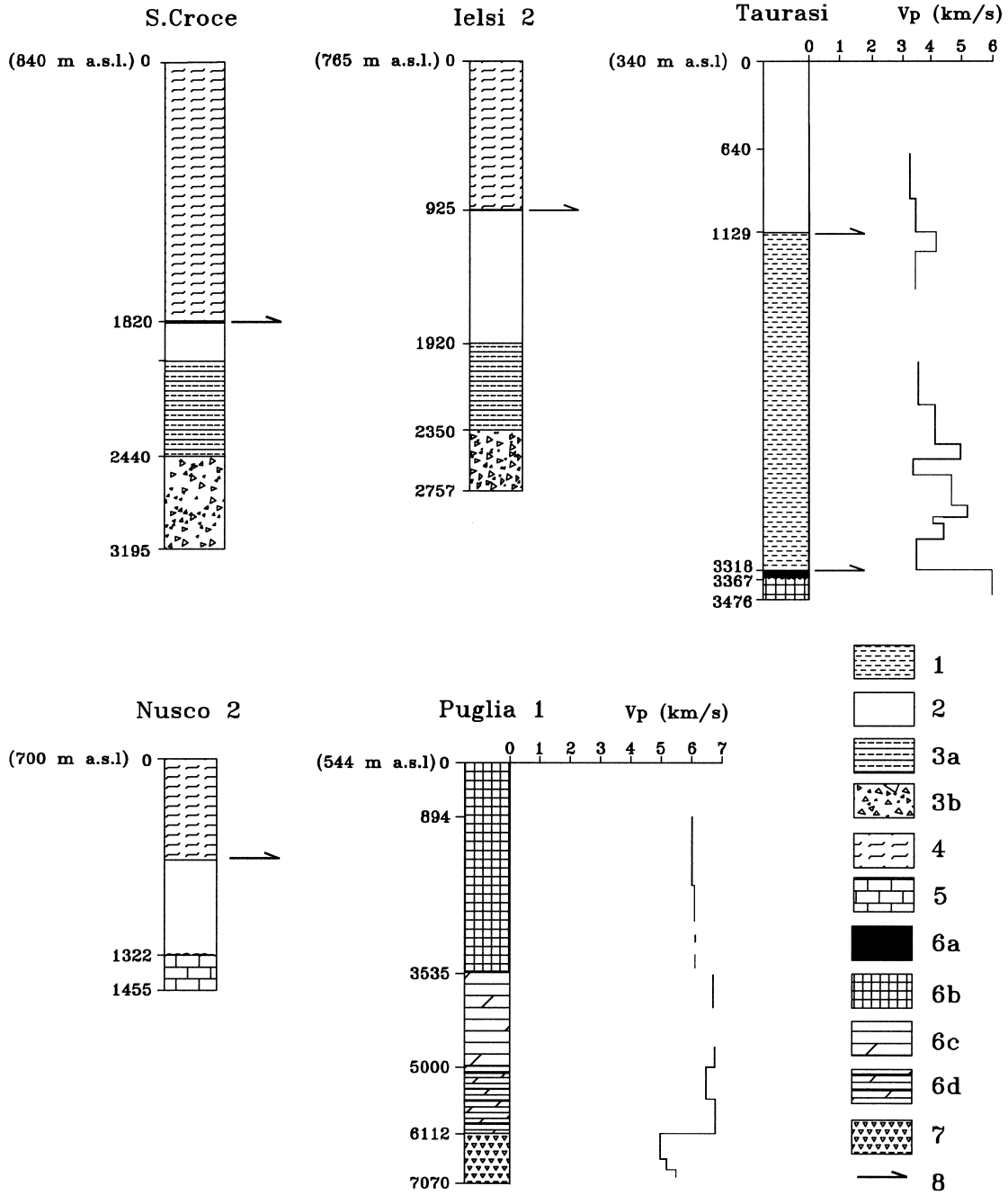


Fig. 2. Stratigraphic and sonic velocity logs from wells located in the Sannio region and in the Apulia foreland. 1 — Late Tortonian–Upper Messinian thrust-sheets-top deposits; 2 — Upper Miocene siliciclastic flysch deposits of the Molise Basin (S. Croce and Ielsi 2 wells) or unconformably overlying the Western Carbonate Platform (Taurasi and Nusco 2 wells); 3 — Molise nappe: (a) clays, marls and marly limestones (Cenozoic upper sequence), (b) dolomitized breccias and calciturbidites (Mesozoic lower sequence); 4 — Paleogene–Lower Miocene varicoloured clays and basinal coarse-clastic lime resediments of the Sannio nappe; 5 — Mesozoic limestones of the Western Carbonate Platform; 6 — Apulia Carbonate Platform: (a) Messinian anhydrites, (b) Cretaceous–Lower Jurassic limestones and dolomit limestones, (c) dolomites of uncertain age, (d) Triassic dolomites and anhydrites of the Burano formation; 7 — Lower Triassic–Permian clastic deposits of the Verrucano formation; 8 — main thrust plane.

6.2 km/s range in the first 3.5 km and velocities in the 6.5–6.7 km/s range from 3500 m to the bottom of the evaporites. From 6112 to 7070 m, a considerable velocity decrease has been observed (average velocities: 5.0–5.5 km/s).

The seismostratigraphic succession described above is confirmed by Gargano 1 well, located 90 km north of Puglia 1 well (Fig. 1); the only relevant difference is a thickening of the Burano evaporites from 1.1 to 2.0 km.

4. Seismic data acquisition and analysis

Seismic data presented in this paper were recorded in 1992 along a main line 75 km long and oriented N 150°. The seismic profile is roughly parallel to the strike of the regional compressive fronts in the Molise–Sannio Apenninic segment (Fig. 1).

Five shots located along the line with a spacing of about 15 km were recorded by a number of seismic stations ranging from 34 to 59 deployed along the profile with a spacing of 1–2 km. A variety of portable 1 and 3 components stations with 1 and 2 Hz seismometers were used. Shot points and seismographs locations are accurate to approximately 50 m (for a detailed description of the 1992 seismic survey, see Iannaccone et al., 1998).

The record seismic sections are shown in the upper panels of Fig. 3a–e. Most of the records display a weakly emergent first arrival (Fig. 3b). Impulsive first arrivals are recorded only at close distances from the shot site. The maximum travel distance where we observe an acceptable signal level is about 40 km from each shot point. The times of the first arrival and of the reflected phase were identified on record sections plotted with different time distance zooms and processed using bandpass filters of different widths. We have interpreted each record section by modelling arrival times of the identified seismic phases with an interactive two-dimensional ray tracing technique based on the asymptotic ray theory (Cerveny et al., 1977). Travel times were fitted to within 0.05 s; in some cases, occasional mismatches up to 0.1 s occur. Since the topography along the profile changes by about 450 m, we include it in the

modelling by adding a delay time at each station computed using a mean subsurface velocity of 3 km/s. This value corresponds to the average velocity value estimated by interpreting the first arrival times observed at the stations closest to the shots.

In performing our analysis, we started by interpreting the P-wave direct arrivals, critical refractions and near vertical reflected arrivals in order to obtain a detailed shallow velocity model about 3–4.5 km deep. Seismic data do not show any indication of remarkable velocity gradients. We estimate, from trial-and-error perturbations of model parameters, that the mismatches between observed and computed arrival times of the seismic phases produce overall velocity variations in the shallow model of approximately 0.1 km/s and interface depth variations of approximately 0.2 km.

The deeper structure has been constructed by modelling reversed refraction and intermediate-angle reflection data; here, we estimate a possible variation of 0.2 km/s in the P-wave velocity value and a depth of about 0.5 km.

5. Results

5.1. Velocity structure of the shallow crust

The modelling of seismic refraction data and the interpretation of the shallow crustal structure, up to a depth of 3–4.5 km are aided by the previously described stratigraphic and sonic velocity logs from oil exploration wells (Fig. 2) and three proprietary commercial seismic profiles that cross the seismic refraction profile. The upper and lower panels of Fig. 3a–e contain, respectively, seismograms and ray-trace models computed for the final P-wave velocity model showed in Fig. 4.

5.1.1. North-western segment (between shots S1 and S4)

The first arrivals recorded at an offset up to 10 km for shots S1, S2, S3 and S4 (phase *d1* in Fig. 3a–d) allow the definition of an upper layer with a velocity of 3.3 km/s. This layer corresponds to the Sannio nappe and the Tertiary portion of

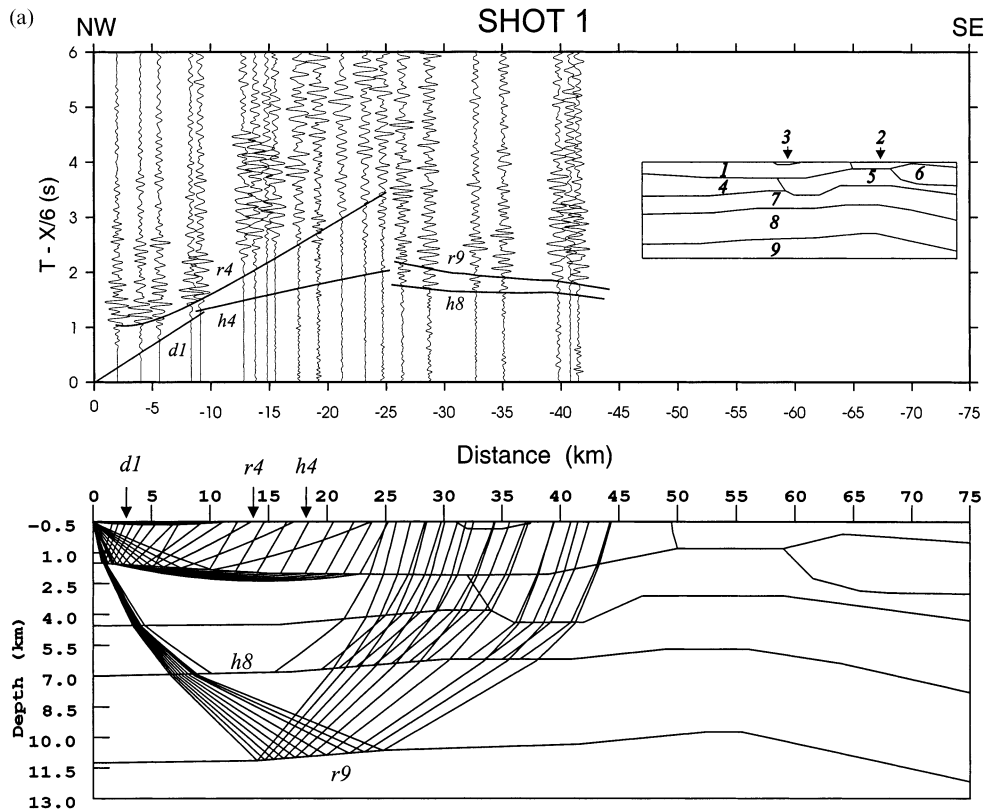


Fig. 3. (a)–(e) Record section for each shot point and seismic model with the indication of ray path for each analysed phase. Data are plotted with normalized amplitude and reduced time scale, with a velocity reduction of 6 km/s. Data have been bandpass-filtered between 5 and 15 Hz. The arrival branches overlapped on data are computed by ray tracing. The small letters and numbers represent, respectively, the type of analysed phase (d =direct, h =head waves, r =reflected) and the layer where the direct phase propagates or the refracted/reflected phase has been generated [see the numbered model in the upper panel in (a)]. The seismic model is shown with vertical exaggeration close to 2. The lower panel of (b) displays a time/distance zoom (grey box in the upper panel) that points out a weakly emergent first arrival.

the Molise nappe (Fig. 4). Evidence for this correlation comes from surface geology (Fig. 1) and from the stratigraphic logs of Ielsi 2 and S. Croce wells (Fig. 2). From seismic data, there is no indication of any seismic discontinuity corresponding to the thrust plane separating the Sannio nappe from the Tertiary portion of the Molise nappe; we suppose, in accordance with the available well and seismic reflection data, that this interface is not marked by a velocity contrast strong enough to be revealed by this seismic refraction survey.

First arrival time delays, within the first 5 km north of shot point S3, indicate the presence of a thin shallow layer with a thickness of 0.35 km and a P-wave velocity of 2.0 km/s (phase $h1$ in Fig. 3c).

This body represents the Middle Pliocene clastic deposits of the Benevento piggyback basin (Fig. 4).

The second layer has a velocity of 4.8 km/s. The top of the layer has a depth of 1.5 km at the northern border and gently deepens to 2.1 km of depth below shot S3 (Fig. 4). The velocity and depth of this layer have been defined by modelling the first-arrival refracted branches observed in the range of 10–25 km for shot S1 and 10–17 km for shots S2 and S3 (phases $h4$ in Fig. 3a–c). The depth of the layer below shots S1 and S2 is also constrained by reflected arrivals at offsets up to 25 km (phases $r4$ in Fig. 3a and b). This body correlates with the Mesozoic dolomitic breccias

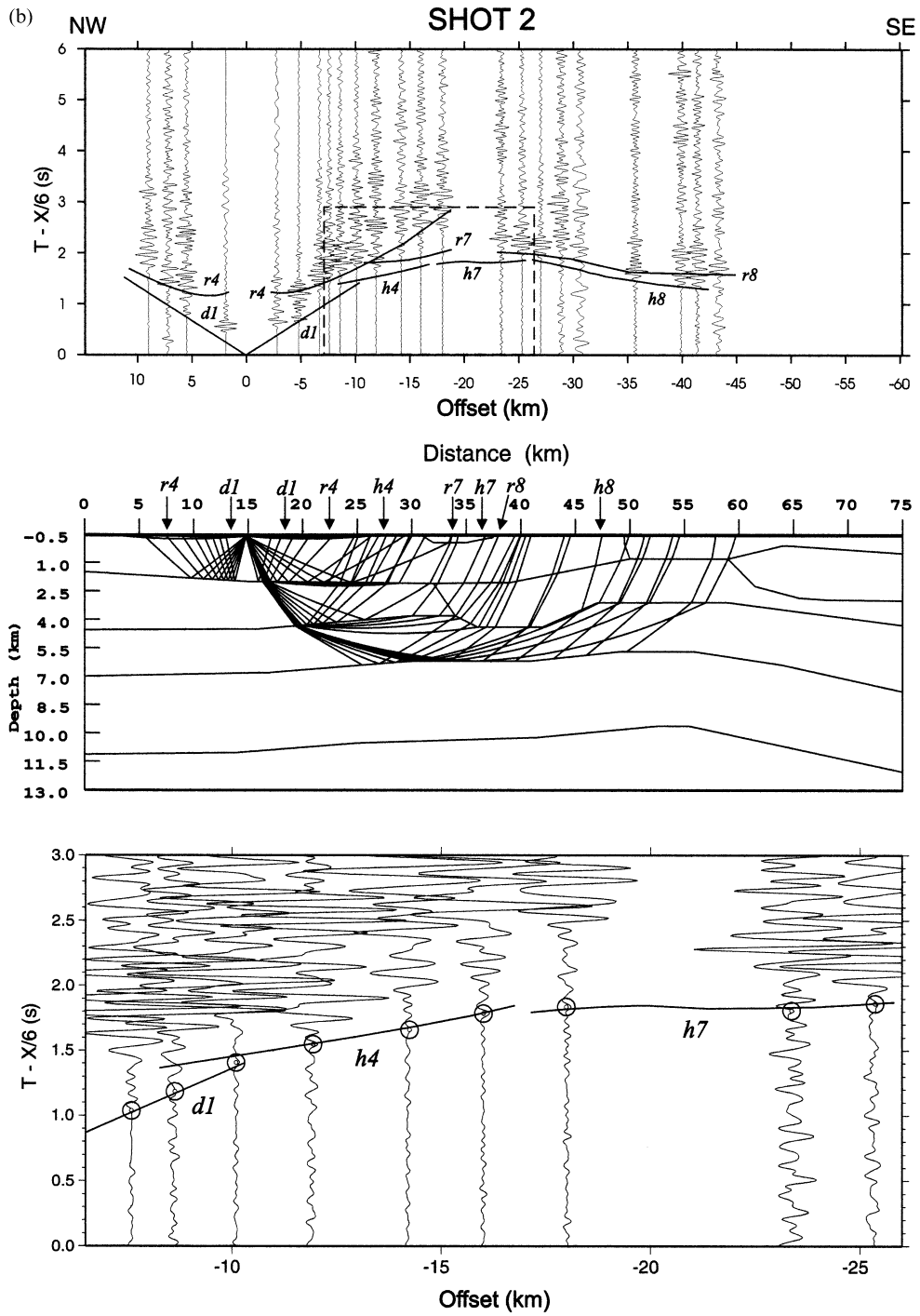


Fig. 3. (continued)

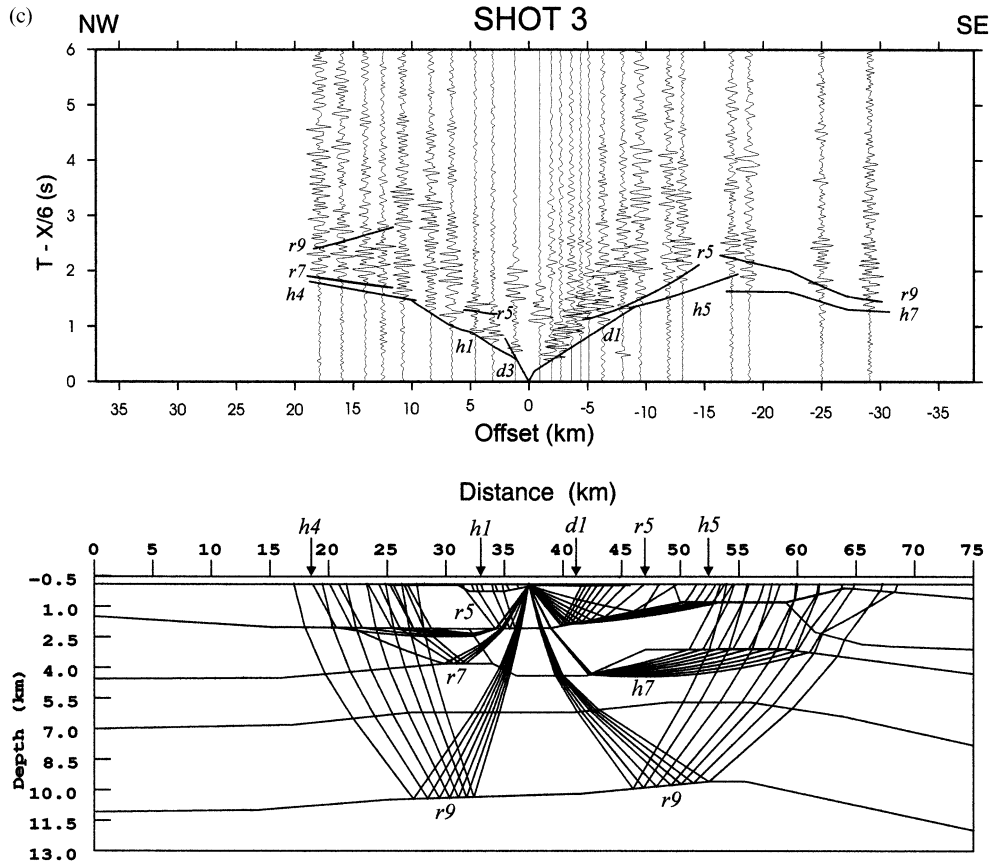


Fig. 3. (continued)

and cherty limestones of the Molise Basin (Fig. 4), as inferred by Ielsi 2 and S. Croce well data (Fig. 2).

5.1.2. Southeastern segment (between shots S4 and S5)

South of shot S4, the velocity model is constrained by the seismic sonic log of the Taurasi 1 well (Fig. 2). A superficial velocity of 2.8 km/s is determined from direct P waves observed at an offset up to 3 km for shots S4 and S5 (phase *d2* in Fig. 3d, Fig. 3e). This value is not confirmed by sonic logs that provide a higher velocity of 3.3–3.5 km/s at a depth of 0.3–0.8 km. The discrepancy between the seismic refraction and well data can be explained by considering that the direct waves, observed at an offset up to 3 km, propagate in the superficial sediments characterized by lower veloci-

ties. Thus, we suggest that the velocity from the value of 2.8 km/s observed at the surface increases with a gradient of 0.6 s^{-1} , reaching a value of about 3.5 km/s at the bottom of the layer located at a depth of 0.8 km.

First-arrival refracted branches with an apparent velocity in the range of 4.1–4.3 km/s have been observed south of shots S3 and S4 (phase *h5* in Fig. 3c and d). These phases define a seismic discontinuity with a velocity of 4.1 km/s at a depth varying from 0.8 to 1.9 km (Fig. 4). Near-vertical reflected arrivals from shot S3 (phase *r5* in Fig. 3c) restrict its depth to between 32 and 47 km along the profile. Sonic logs from the Taurasi well confirm a velocity discontinuity of 3.5–4.1 km/s at a depth of 0.8 km, but they also show below this interface a chaotic succession of low-velocity (3.4–3.6 km/s) and high-velocity (4.1–5.2 km/s)

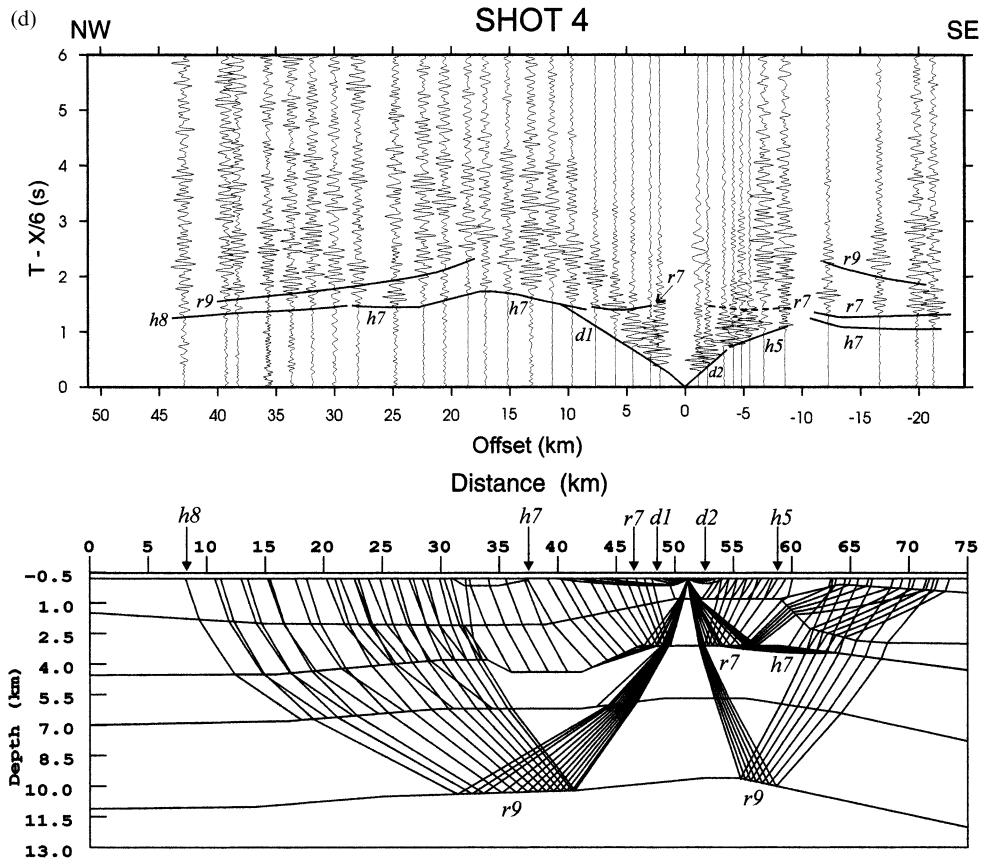


Fig. 3. (continued)

intervals down to 3.0 km depth, which are not detected by seismic refraction data probably because of the receivers' spacing. Thus, we assign a velocity value of 4.1 km/s to the whole succession, corresponding to the average velocity deduced from the sonic log. According to stratigraphic well log information, it has been interpreted as a Late Tortonian–Upper Messinian chaotic and/or deeply deformed sedimentary complex tectonically overlain by Upper Tortonian siliciclastic flysch deposits, the latter corresponding to the 2.8–3.5 km/s interval (Fig. 4).

A prominent shallow feature of the model is a high-velocity wedge, with a velocity of 6.0 km/s, overlying the 4.1 km/s body between 58 and 75 km (Fig. 4). The velocity and horizontal dimension of the wedge are determined from the refracted first arrivals from shot S5 (phase *h6* in Fig. 3e) and by

data of Nusco 2 well (Fig. 2). Moreover, the presence of this high-velocity body is also suggested by the early refracted and reflected arrivals from shots S3 (phases *h7* and *r9* in Fig. 3c) and S4 (phases *h7* and *r7* in Fig. 3d). This body is interpreted as a major thrust sheet formed by limestones of the Western Carbonate Platform (Fig. 4). The primary evidence for this correlation comes from the stratigraphic log from Nusco 2 well (Fig. 2).

5.2. Deep model

The 4.1 and 4.8 km/s bodies overlie a continuous layer, about 2.5 km thick, with a velocity and gradient of 6.0 km/s and 0.07 s^{-1} , respectively (Fig. 4). The velocity, gradient and depth (varying from 3.0 to 4.5 km) of the layer are determined

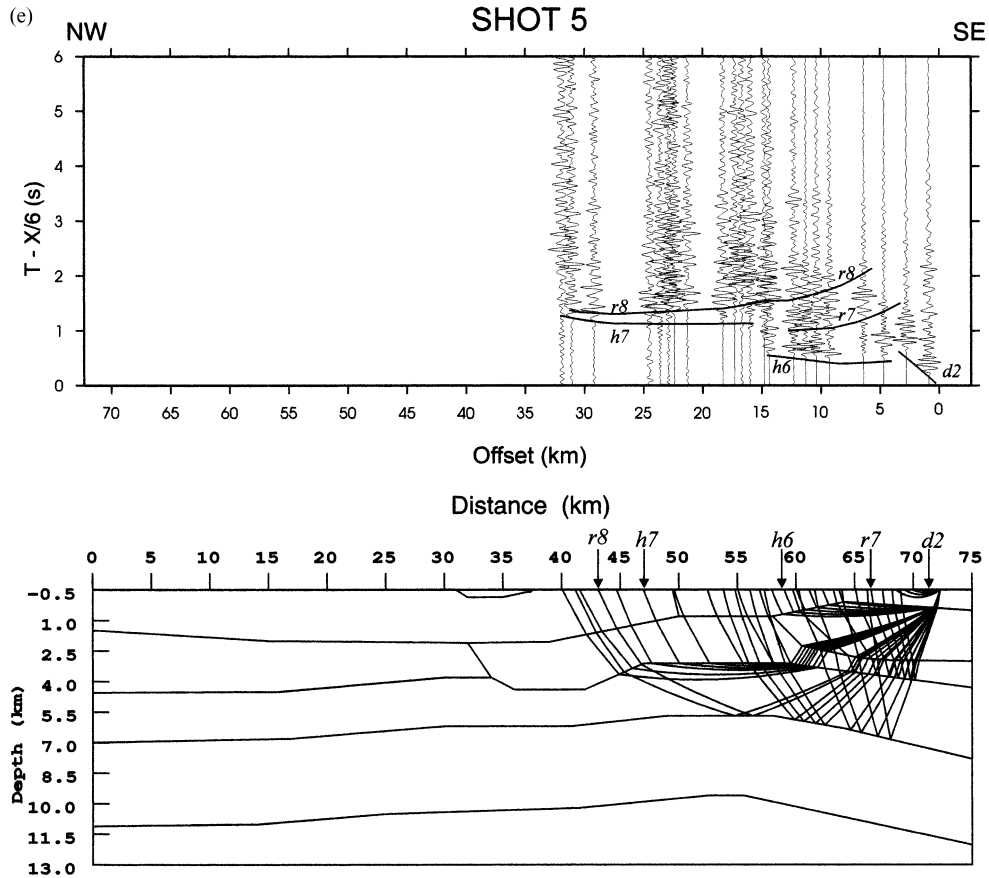


Fig. 3. (continued)

primarily from the first-arrival refracted branches, with apparent velocities in the 5.5–6.5 km/s range, observed south of shots S2, S3 and S4 and north of shots S4 and S5 (phases *h7* in Fig. 3b–e). South of shot point S2, the top of the layer is extremely well constrained because refracted rays from shots S2, S3, S4 and S5 illuminate the same part of the model, and near-vertical reflected arrivals from the same shots (phase *r7* in Fig. 3b–e) provide additional constraints on its depth. Moreover, sonic logs of the Taurasi well also display an abrupt increase in velocity from 3.6 to 6 km/s at a depth of 3 km (Fig. 2). North of shot point S2, the corresponding arrivals from shot S1 are not observed probably because the amplitude of the refracted phase is not large enough to overcome the noise level. The depth of the layer between 0

and 18 km is constrained by a proprietary commercial seismic profile. The 6.0 km/s layer corresponds to the Meso-Cenozoic deposits of the Apulia Carbonate Platform drilled by the Taurasi well at a depth of 3 km (Fig. 4) and explored by several commercial boreholes east of the seismic refraction profile, as shown in Section 7 (Fig. 7a–c).

A second layer, with a velocity of 6.6 km/s occurs at depths of 6–7 km (Fig. 4). It is determined by critically refracted arrivals branches observed south of shot points S1 and S2 and north of shot point S4 (phase *h8* Fig. 3a, b and d), with an apparent velocity in the 6.3–6.9 km/s range, and by intermediate angle reflections from shot S2 and S5 (phase *r8* in Fig. 3b and e). On the basis of subsurface data from Puglia 1 (Fig. 2) and Gargano 1 wells located in the Apulia foreland

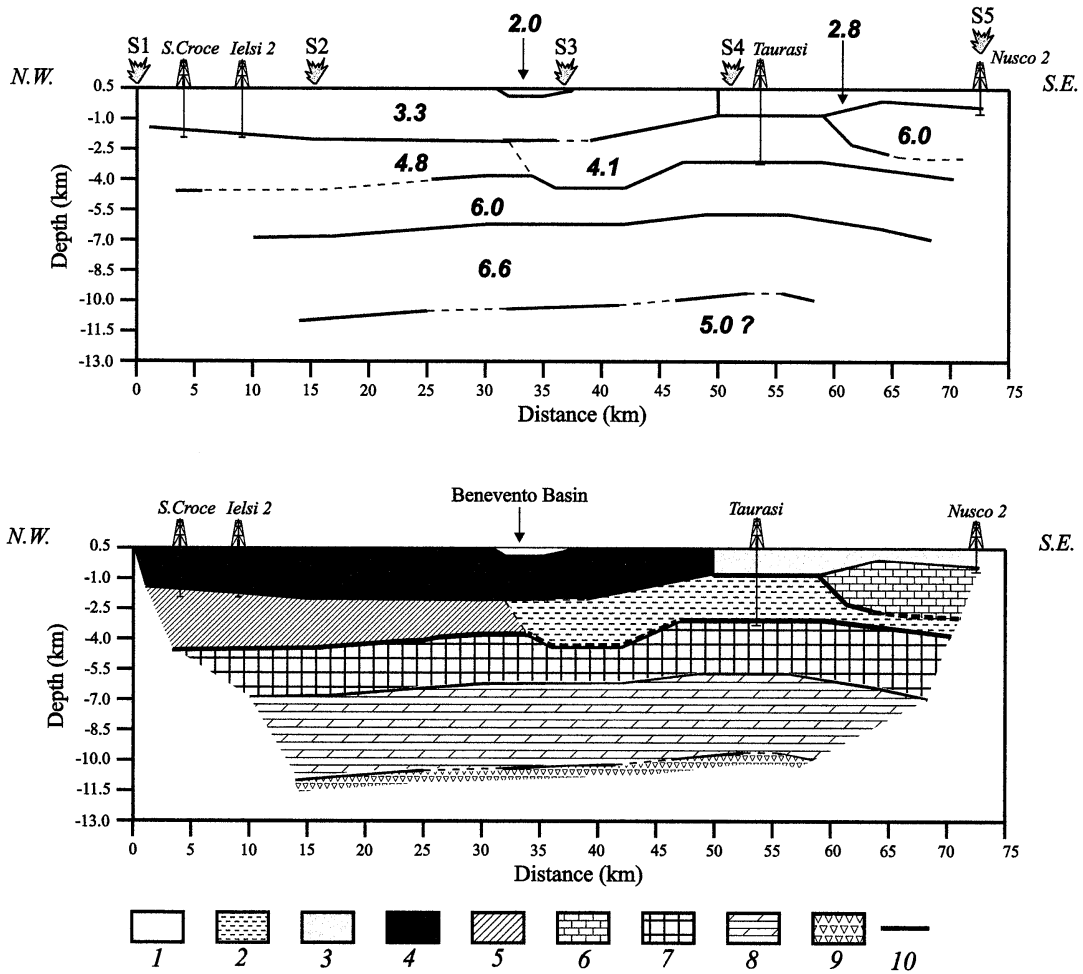


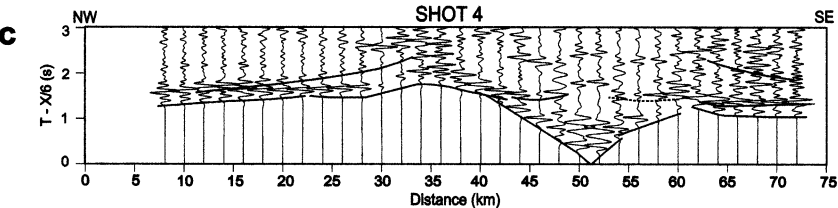
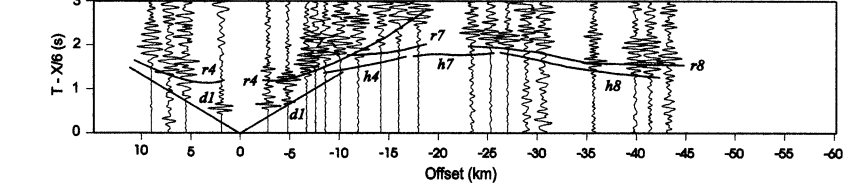
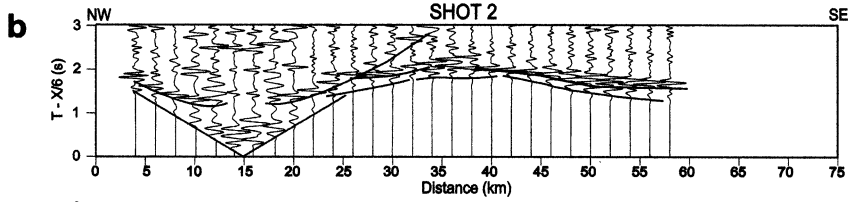
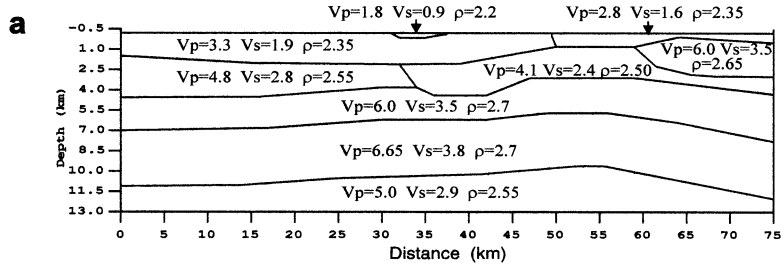
Fig. 4. Upper panel: final P-wave velocity model. Thick continuous lines correspond to the seismic interfaces investigated by seismic rays, and dashed lines refer to extrapolated interfaces; numbers indicate P-wave velocity values. Shot points and wells are also shown. Lower panel: geological interpretation of the P-wave velocity model. 1 — Middle Pliocene clastic deposits of the Benevento basin; 2 — Late Tortonian–Messinian thrust-sheets-top deposits; 3 — Upper Miocene flysch deposits unconformably overlying the Western Platform carbonates; 4 — Sannio and Molise nappes (Cenozoic upper sequence); 5 — Molise nappe (Mesozoic lower sequence); 6 — Western Carbonate Platform (Meso-Cenozoic limestones); 7 — Apulia Carbonate Platform (Jurassic–Tertiary limestones); 8 — Apulia Carbonate Platform (Upper Triassic dolomites and anhydrites of the Burano formation); 9 — Verrucano formation (Permo-Triassic clastic deposits); 10 — main thrust planes, as suggested by Taurasi well data and by previous structural models of the region.

(Fig. 1), it has been interpreted as a second-order discontinuity of the Apulia Carbonate Multilayer.

The deepest detected seismic discontinuity occurs at depths of 9–11 km (Fig. 4). Its morphology is determined by intermediate–wide angle reflected arrivals for all shots except S2 (phase $r9$ in Fig. 3a, c and d). The velocity below this interface is unconstrained, but we try to assign a velocity value to the deepest interface by modelling

the amplitude of the reflected arrivals by finite difference simulations, as described in the following paragraph.

As shown in Fig. 1, our seismic profile was located in a region with a strong structural variation in the SW–NE direction, perpendicular to the seismic line. From the structural models proposed for the southern Apennines, we assume a maximum dip of the layers of 20° in the SW direction.



We estimate that the incertitude on the depth of each layer is about 6% of their value.

6. Finite difference waveform modelling

Complete synthetic seismograms for all the analysed sections have been produced by the 2-D elastic finite difference method (Graves, 1996) in order both to check the reliability of the velocity model inferred by ray-tracing modelling of first and reflected arrivals times, and to model amplitude of the reflected arrivals from the deepest interface. The model used to produce synthetic seismograms is shown in Fig. 5a. The S-wave velocity values have been computed using a V_p/V_s ratio value of 1.73 for all the layers except the superficial layer, located north of shot S3 and corresponding to the Benevento basin (mainly formed by soft clays), where we used a V_p/V_s ratio of 2. The density values used for each layer are deduced by gravity modelling described in the following paragraph. The investigated section is 75 km long and 13 km deep. A grid spacing for the simulations of about 13 m has been chosen in order to obtain accurate waveforms up to 10 Hz for the given velocity model. Absorbing boundary conditions have been used on all sides of the grid, adding a 2.5 km thick border, except at the free surface where stress-free conditions are applied (Levander, 1988).

Fig. 5b, c and d compare the synthetic and observed velocity seismograms for common shot gathers S2, S4 and S5. Both synthetic and observed sections have been bandpass-filtered between 4 and 10 Hz. The low-frequency cut-off is needed because of noise in the observed recordings; the high-frequency cut-off is applied because of the high-frequency limit in the simulations.

Overall, the synthetic and observed sections match fairly well, especially concerning the pre-

dicted arrival times of primary and dominant reflected phases. The model explains the small amplitude of first arrivals, mostly consisting of head waves, compared to the large amplitude of early and late reflected waves at offsets larger than 5 km. However, in some cases, synthetics do not reproduce the relative amplitude correctly among early and late reflected arrivals (phases $r4$ and $r7$ in Fig. 5b), and the model appears too simple to reproduce real data complexity mainly ascribed to the surface waves propagation.

The record section relative to shot S4 (Fig. 5c), which explores the total profile length, displays reflected arrivals from the deepest interface of the model (phase $r9$). The velocity below this interface is unconstrained by the ray-tracing modelling. However, the large amplitudes of the reflected arrivals suggest an important impedance contrast at the reflecting boundary. Polarity of this reflected phase appear confuse due to the high noise level of the seismograms and cannot be used to discriminate the velocity contrast.

We performed several finite difference simulations varying the velocity and density values below this interface. Our modelling confirms that very large ($V_p > 7.5$ km/s) or small ($V_p < 5.0$ km/s) velocity values are needed to generate reflections with an amplitude comparable to real data. The synthetic seismograms shown in Fig. 5c have been produced by assuming a velocity value of 5.0 km/s. We prefer to hypothesize a strong velocity inversion (from 6.6 km/s to 5.0 km/s) at the reflecting interface because a P-wave velocity value larger than 7.5 km/s is typical of lower crustal rocks and cannot be considered realistic at this depth in the Southern Apennines. In fact, the lower crust appears not to be involved in the thrusts and folds system of the accretionary wedge, as suggested by gravity and magnetic data (Corrado and Rapolla, 1981; Agip, 1982).

Our synthetics also reproduce the observed wide

Fig. 5. Finite difference waveform modelling. (a) Velocity and density models used for finite difference simulations. (b–d) Synthetic seismograms (upper panel) and record sections (bottom panel) for shots S2 (b), S4 (c) and S5 (d). Both synthetic and real data are plotted with a normalized amplitude and reduced time scale ($V_r = 6.0$ km/s) and have been bandpass-filtered between 4 and 10 Hz. The arrival branches overlapped on data are computed by ray tracing; the small letters and numbers in the bottom panels indicate the type of analysed phase (see Fig. 3a).

angle amplitude increase of the reflected arrivals towards northwest. We note the predicted amplitude decrease of the first refracted arrivals north of the shot point at an offset between 14 and 23 km (phase *h7*), which is an effect of the complex morphology of the 6.0 km/s interface.

Synthetics for shot S5 (Fig. 5d) match well with the large amplitude of the reflected arrivals from the 6.6 km/s discontinuity (phase *r8*). Moreover, finite difference simulations reproduce the first arrival times and waveforms observed about 15 km north of the shot point (which we could not model by ray-tracing) and allow these arrivals to be explained in terms of diffractions generated by the high velocity (6.0 km/s) wedge located in the southernmost part of the investigated profile (Fig. 4). In conclusion, although the model inferred by seismic refraction data appears too simple to completely reproduce real data complexity by difference finite simulations, overall, the synthetic and observed sections match well, showing the usefulness of the finite difference tool to check our model.

7. Gravity data modelling

With the aim of checking the reliability of the inferred velocity model, we verified its consistency with respect to another physical observation: the gravity field. The gravity data covering the investigated region were collected by several institutions and universities. We extracted from this database (Carrozzo et al., 1981) about 12000 gravity stations. The spatial distribution of the gravity stations was not homogeneous as a consequence of the rugged topography of the western part of the Sannio region. However, an average density distribution of about 1.5 stations per km² was available. All the gravity data are referred to the IGSN71 network (Morelli et al., 1974). Free-air and Bouguer corrections were performed referring to the sea level, and terrain corrections, applied to account for the gravitational effect of the topography, were extracted from the database. Bouguer anomalies were computed, with reference to the 1980 International Ellipsoid, using $\rho = 2400 \text{ kg/m}^3$ as reduction density, an average value considered to be representative of the rocks density in the

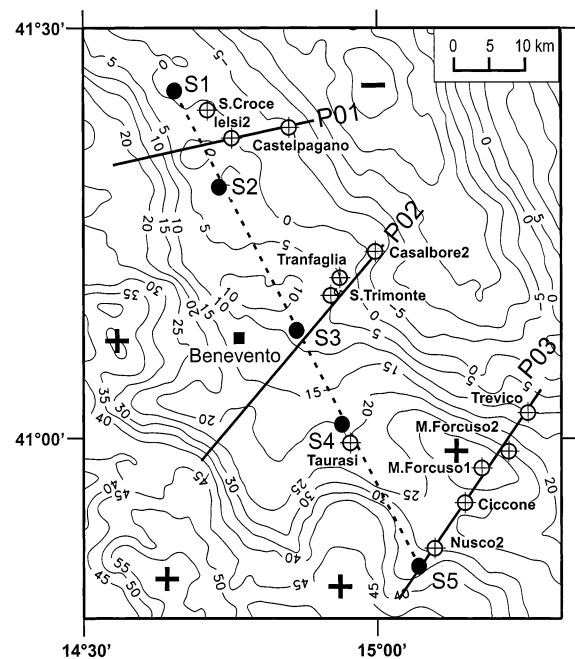


Fig. 6. Bouguer anomalies of the northern sector of the Southern Apennines thrust belt, computed using 2400 kg/m^3 as reduction density. The contour interval is 5 mGal; + and – indicate the relative maximum and minimum of the anomaly. The traces of the interpreted profiles (continuous line), location of the wells (open circle), the refraction line (dashed line) and shot points (solid circles) of the 1992 seismic survey are also shown.

area, as can be inferred from surface geology and well data. Fig. 6 shows the Bouguer anomaly map contoured at 5 mGal intervals, ranging from –30 to 60 mGal with a general decreasing trend of the values from SW to NE, at a mean rate of 1.1 mGal/km, mainly due to the deepening of the Moho boundary from the Tyrrhenian to the Adriatic margin. Generally, relative maxima are related with outcrops of the Western Carbonate Platform or with nappes anticline deforming the Apulia Carbonate Platform, while relative minima are related to Plio-Pleistocene basins. In particular, the minimum located in the north-eastern part of the investigated area is related to the Bradano foredeep (Fig. 1). The Bouguer anomaly map displays a complex pattern due to the presence of anomalies of different wavelengths, related to the different depth of the gravity sources. In order to enhance the major features related to the subsur-

face structures, we have separated the Bouguer anomaly into components with a different frequency content, using a two-dimensional low pass filter in the wave number domain. Several authors (Mishra and Pedersen, 1982; Chakraborty and Agarwal, 1992) generalize to Bouguer anomaly data analysis, the spectral technique developed by Spector and Grant (1970), who first supplied a method to estimate the mean depth of a magnetic susceptibility discontinuity surface, based on a statistical analysis of aeromagnetic anomalies performed in the wave number domain. However, our quantitative interpretation is based on the total anomaly, using the filtered maps only to infer main trends not obvious in the original data, such as the relatively low gradient immediately SSE (elongated to the south) of the Benevento town, for example. This relative minimum can be related, according to the velocity model (Fig. 4), to a flexure of the 6.0 km/s layer (corresponding to the Apulia Carbonate Platform) between shot points S3 and S4.

The modelling of the Bouguer anomalies was performed by two-and-a-half forward modelling (Won and Bevis, 1987), that is a modified version of Talwani's algorithm (Talwani et al., 1959). We chose three profiles crossing both the seismic refraction profile and the main trend of the Bouguer anomaly (Fig. 6); for this last reason, we did not perform a gravity modelling along the refraction line. Gravity modelling was constrained by the seismic model previously described, well information, commercial seismic profiles and superficial geology. Starting density values were chosen, using both the reference values proposed by Mostardini and Merlini (1986) and the density–velocity relationship proposed by Nafe and Drake (1963). Finally, the density values used for the geological formations are: 2700 and 2650 kg/m³ for the limestones of the Apulia and the Western Carbonate Platforms, respectively, 2550 kg/m³ for the Mesozoic lower sequence of the Molise Basin; 2500 kg/m³ both for the Late Miocene thrust-sheets top deposits drilled in Taurasi well and for the Cenozoic deposits, mainly consisting of redeposited carbonates, of the Sannio nappe; 2350 kg/m³ for the Cenozoic deposits, mainly consisting of clays, of the Molise Basin and Sannio

nappe, and for the Upper Miocene flysch deposits; and 2200 kg/m³ for the Pliocene basins.

Fig. 7 shows the gravity modelling along the three selected profiles, crossing the refraction line in the northern (P01, Fig. 7a), central (P02, Fig. 7b) and southern (P03, Fig. 7c) part. Profile P01 was constrained both by the analysed seismic refraction profile and by a commercial seismic line in the SW part, Ielsi 2 well (previously described) in the central part and Castelpagano well (Mostardini and Merlini, 1986) in the NE part. Profile P02 was constrained by a commercial seismic line in SW margin, the analysed refraction profile in the central part and three wells (described by Mostardini and Merlini, 1986) in the NE part. Profile P03 was constrained by the analysed refraction line and Nusco 2 well (previously described) in the SW margin, and by four wells (described by Mostardini and Merlini, 1986) in the central and NE parts.

The gravity models are consistent with the velocity and geological sections inferred by interpreting seismic refraction and well data. Furthermore, they allow to constrain the average density value of the geological formations of the investigated area. Moreover, this two-and-a-half forward gravity modelling contributes to an integration of the structural model, extending it in 3D, as discussed in the following paragraph dealing with structural implications.

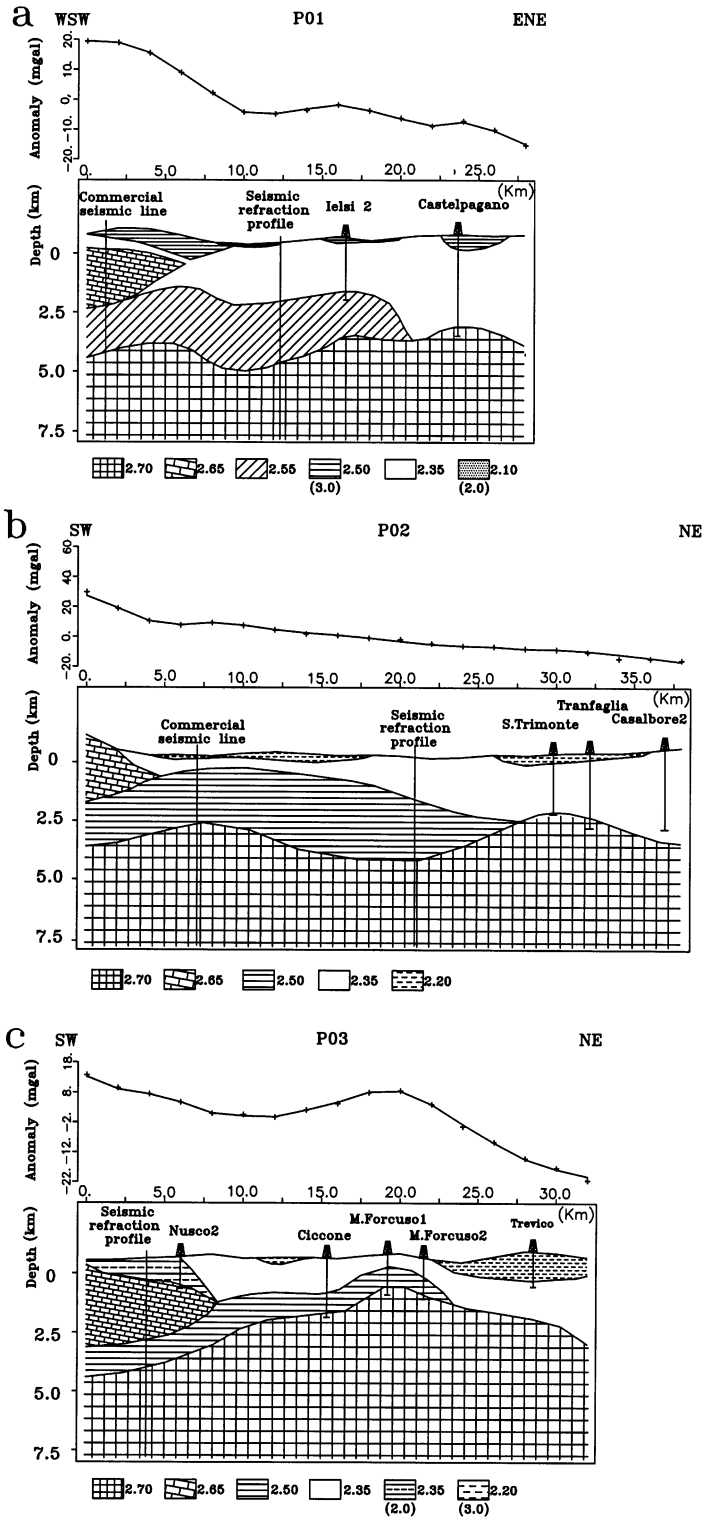
8. Discussion

8.1. Meaning and reliability of the deep seismic discontinuities

8.1.1. Discontinuity 6–7 km deep

The seismic discontinuity characterized by a velocity of 6.6 km/s and 6–7 km deep (Fig. 4) has been interpreted as an inner lithological transition within the Apulia Carbonate Platform, between the Jurassic–Cretaceous carbonates and the Upper Triassic dolomites and evaporites of the Burano formation (Fig. 4), on the basis of the following observations:

Stratigraphic and sonic logs from Puglia 1 (Fig. 2) and Gargano 1 wells, located in the Apulia foreland, display an increase of seismic



velocity from 6.2 to 6.7 km/s in correspondence with the lithological transition from the Jurassic–Cretaceous limestones and dolomitic limestones to the Upper Triassic dolomites and evaporites of the Burano formation.

Subsurface data for oil exploration and seismic refraction surveys performed in Central Apennines confirm that the dolomites and evaporites of the Burano formation have extremely high velocities (6.2–6.8 km/s) (Bally et al., 1986). As inferred by studies on seismic velocities of rocks from laboratory measurements (Christensen, 1982), a velocity value of 6.6 km/s is within the seismic velocity range (6.5–6.9 km/s) found for dolomites at depths of 6–7 km. Alternatively, the 6.6 km/s velocity value could be related to high-grade metamorphic rocks, and this seismic discontinuity could represent the top of a Paleozoic metamorphic basement hypothesized at the bottom of the sedimentary cover. This alternative hypothesis, proposed by Chiarabba and Amato (1997) to explain the high-velocity zones ($V_p \sim 6.3$ km/s) detected in their tomographic model, is in contrast with the information inferred from magnetic data (Agip, 1982), showing no involvement of a relatively shallow (6–7 km deep) metamorphic basement in the thrusts and folds system of the Southern Apenninic accretionary wedge.

8.1.2. Discontinuity 9–11 km deep

The deepest discontinuity, located at a depth of 9–11 km, has been detected by intermediate–wide-angle reflected arrivals. Finite difference simulations performed to model the observed amplitude suggest the existence of a strong velocity inversion at the reflecting boundary. In order to understand the reliability of this seismic discontinuity and to

provide a geological interpretation, we have analysed well data and seismic reflection profiles for oil exploration located in Apulia foreland and Bradano foredeep (Figs. 1 and 8), trying to relate the structures investigated east of the Apenninic chain with those detected in the Sannio region. As result, we interpret the interface 9–11 km deep as a lithological transition from high-velocity (about 6.5–6.7 km/s) Upper Triassic evaporites of Burano formation to low-velocity (about 5.0 km/s) Middle Triassic–Upper Permian clastic deposits of the Verrucano formation (Fig. 4). This hypothesis is mainly supported by two observations:

(1) Sonic logs from Puglia 1 (Fig. 2) and Gargano 1 wells display a strong decrease in velocity from 6.7 to 5.0 km/s at a depth of about 6 and 4.3 km, respectively, in correspondence with the Burano–Verrucano boundary.

(2) Seismic reflection profiles for oil exploration, recorded in the Apulia foreland and Bradano foredeep, show that the upper and lower limits of the Apulia Carbonate Platform coincide with two strong reflectors: the upper at the boundary with the Pliocene–Pleistocene terrigenous marine deposits and the lower at the Burano–Verrucano boundary (Fig. 8). Proceeding from the Apulia foreland to the Bradano foredeep, these horizons run parallel and progressively become deeper because of the Apulian lithosphere flexure. As shown in the seismic reflection profile located at the eastern boundary of the thrust belt (Fig. 8b), the lower strong reflector occurs at times increasing from 4.5 to 5.5 s. A depth conversion of this profile, located about 40 km east of the seismic refraction profile, results in a reflecting interface occurring at increasing depths from about 10 to 11.5 km. Unfortunately, in the central part of the thrust belt, this reflector has no longer been detected by commercial seismic profiles because seismic data

Fig. 7. Gravity modelling across the profiles P01(a), P02 (b) and P03 (c). On top of each model, the observed Bouguer anomaly (crosses) and the calculated anomaly (continuous line) are shown; the optimized density model is displayed at the bottom [density in g/cm^3 , half-length used for the two-and-a-half forward modelling (numbers in brackets) in km]. Wells, commercial seismic lines and the refraction profile constraining the models are shown. (a) 2.70=Apulia Carbonate Platform; 2.65=Western Carbonate Platform; 2.55=Molise nappe (Mesozoic lower sequence), 2.50=Sannio nappe (mainly redeposited carbonates); 2.35=Sannio nappe (mainly clays), Molise nappe (Cenozoic upper sequence), flysch deposits; 2.10=Pleistocene deposits. (b) and (c) 2.70=Apulia Carbonate Platform; 2.65=Western Carbonate Platform; 2.55=Molise nappe (Mesozoic lower sequence), 2.50=Late Miocene thrust-sheets deposits; 2.35=Sannio nappe, Molise nappe (Cenozoic upper sequence), flysch deposits; 2.20=Pliocene basins.

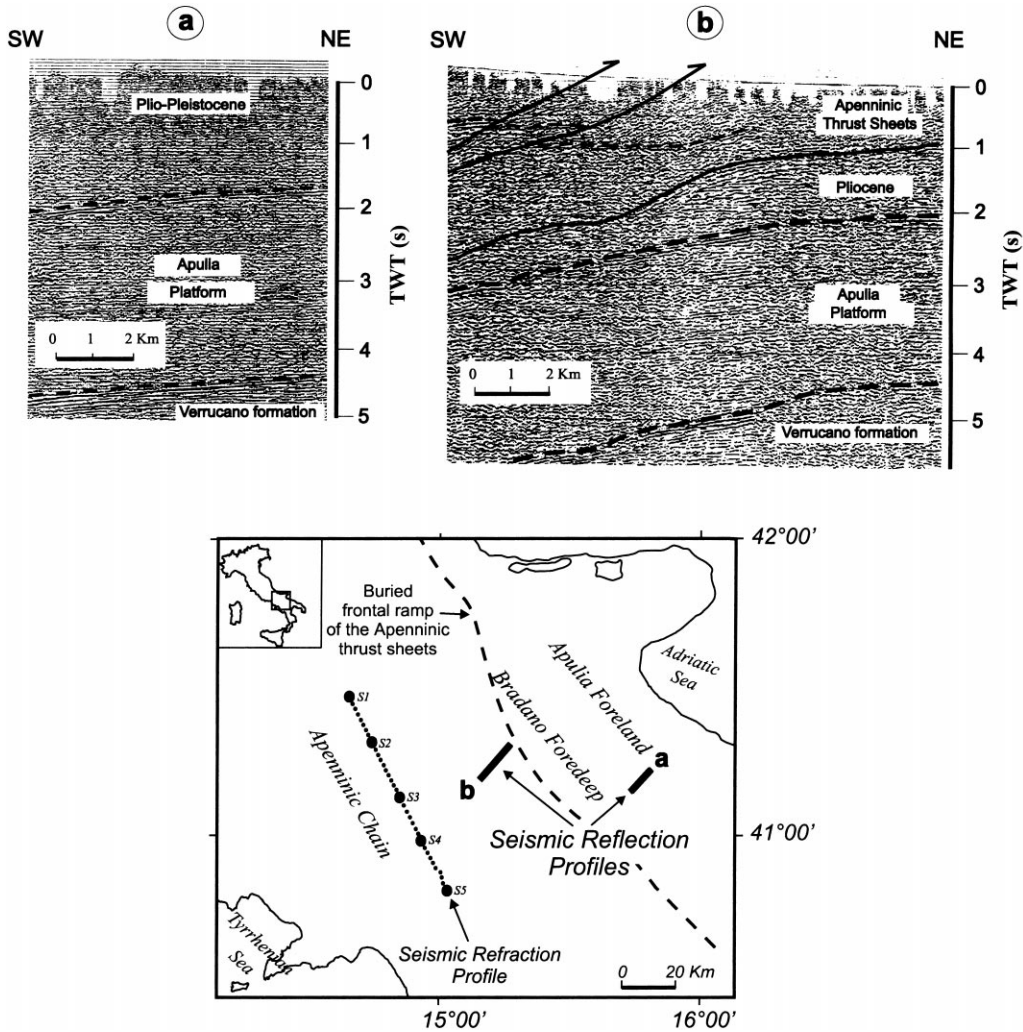


Fig. 8. Seismic reflection profiles for oil exploration located in the Apulia Foreland (profile a) and Bradano Foredeep (profile b) (modified from Roure et al., 1991). Note the strong reflectors at 1.6–2.0 s TWT (profile a) and 2.0–3.0 s TWT (profile b), corresponding to the discontinuity between Pliocene terrigenous marine deposits and carbonates of the Apulia Platform. The strong markers at about 4.5 s TWT on profile a and 4.5–5.5 s TWT on profile b represent the bottom of the Apulia Carbonate Platform; as suggested by subsurface data from the Puglia 1 well, this reflector corresponds to the Burano–Verrucano boundary, characterized by a strong decrease in P-wave velocity values.

are of poor quality, especially beneath the top of the Apulia Carbonate Platform, and generally are not processed deeper than 6 s. In any case, at the eastern boundary of the thrust belt, the deep strong reflector (corresponding to the Burano–Verrucano boundary) occurs at depths (10–11.5 km) comparable with those (9.5–11 km) hypothesized in the Sannio region on the basis of the seismic refraction profile interpretation.

Likewise, in Central Italy, low-velocity (about 4.0 km/s) Permian clastic deposits and Triassic phillites of the Verrucano formation have been drilled below Mesozoic carbonates and Burano evaporites. Seismic reflections profiles, calibrated using both surface and well data, show that the top of the Permo-Triassic sequence corresponds to a deep strong reflector that can be followed from the Adriatic coast to the interior Central

Apennines down to a depth of about 10 km (Bally et al., 1986).

Moreover, an electrostratigraphic section obtained by a magnetotelluric survey recently performed along a profile crossing the Apenninic chain from the Adriatic sea to the Sele plain (Fig. 1) seems to confirm the continuity of the Verrucano formation. In fact, the MT section that is constrained in the eastern part by Puglia 1 well in the Bradano foredeep displays, below a high resistive layer (corresponding to the Apulia Carbonate Platform), a continuous conductive layer, about 2 km thick, which could be related to the clastic deposits of the Verrucano formation (Marsella et al., 1998).

8.2. Structural implications

Geological interpretation of the 2-D velocity model, well data analysis and gravity data modeling provide some interesting indications about the upper-crustal structure of the northern sector of the Southern Apennines. The shallower part (upper 4 km) of the velocity model appears more homogeneous in the north-western sector than in the south-eastern sector (Fig. 4). The fairly regular layering observed north of shot S3 can be explained, considering that in the northwestern sector, the seismic line (azimuth 150°) runs parallel to the NNW–SSE compressional structures of the Molise–Sannio arcuate segment; conversely, in the southeastern sector, the line cuts the WNW–ESE compressive fronts of the Campania–Lucania arcuate segments (Fig. 1). Thus, south of shot S3, the velocity model displays strong lateral heterogeneities produced by the overlapping of different thrust sheets. A major thrust sheet formed by the Western Carbonate Platform and Upper Miocene flysch deposits overlies the Late Miocene chaotic and/or deeply deformed sedimentary complex drilled in Taurasi well; the latter overthrusts above the top of Apulia Carbonate Platform that coincides with the roof thrust of the Southern Apennines duplex system (Fig. 4). The shallow crustal structure is better documented by all the gravity sections because they strike normal to the compressional structures of the investigated area (Fig. 6). The gravity sections P02 and P03 clearly display the

structural pattern described before (Fig. 7b, Fig. 7c); conversely, the gravity section P01, which cuts the Molise–Sannio arcuate segment, shows the Molise nappe sandwiched between the Western and the Apulia Carbonate Platforms (Fig. 7a).

The irregular morphology of the top of the Apulia Platform, which reaches a minimum depth of 0.3 km in correspondence with the M. Forcuso 1 well (Fig. 7c), is interpreted as a consequence of contractional structures. In particular, the nappe anticline and syncline deforming the Apulia carbonates along the seismic refraction profile between shot points S4 and S3 (Fig. 4) can be interpreted as structures developed above a ramp thrust and flat thrust, respectively; the latter could also explain the presence of the Middle Pliocene Benevento basin located north of shot point S3. These structural features are extremely well displayed in the P03 gravity section (Fig. 7c). The nappe anticline explored by M. Forcuso 1, M. Forcuso 2 and Ciccone wells could result from the emplacement of a thrust ramp in the underlying Apulia carbonates, whereas the nappe syncline and the Upper-Middle Pliocene piggyback basin drilled by Treviso well could be linked to the flat.

Tectonic thickening due to the thrust faulting can explain the large thickness (about 6.5 km) of the Apulia Carbonate Multilayer (Fig. 4). The evaporites and dolomites of the Burano formation may reach a thickness of about 4 km. A comparison of this value with that observed in the wells located in the Apulia foreland (1–2 km) suggests that the Burano anhydrites are deeply involved in the tectonic shortening.

Finally, the parallel trend of the top of the Apulia Carbonate Platform and Verrucano formation (Fig. 4) suggests that the latter has been involved in compressional tectonics too. Thus, the sole thrust of the Southern Apennines thrust belt does not coincide with the bottom of the Burano anhydrites, as proposed by Mostardini and Merlini (1986) and Roure et al. (1991), but it is deeper within the sedimentary Paleozoic strata.

8.3. Comparison with previous crustal models

The structural model of the Southern Apennines proposed by Mostardini and Merlini (1986) is

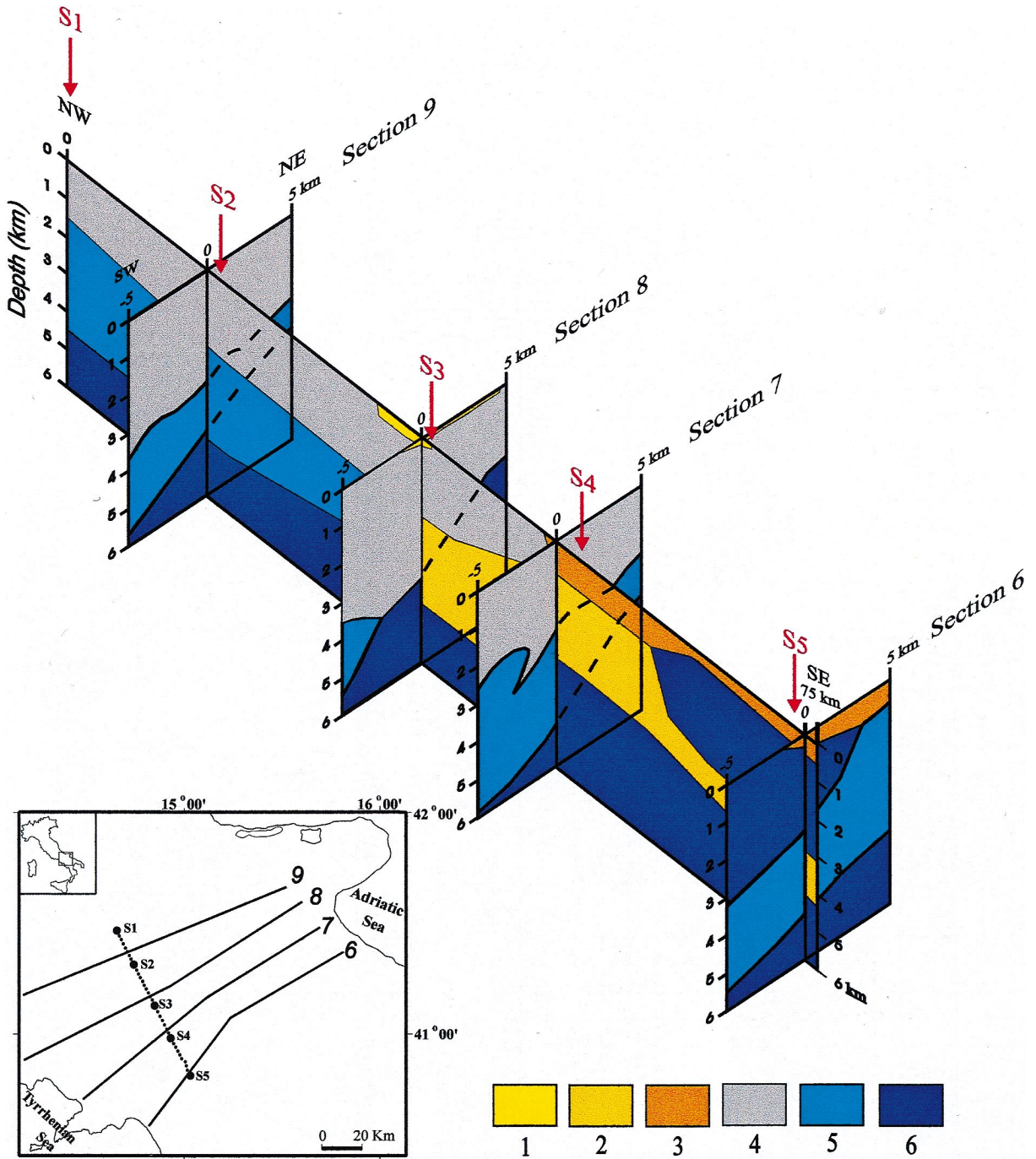


Fig. 9. Comparison of the proposed model with four geological sections from Mostardini and Merlini (1986). The location of the four cross-sections is shown in the box. 1 — Middle Pliocene deposits; 2 — Late Tortonian–Upper Messinian thrusts-sheets-top deposits; 3 — Upper Miocene flysch deposits unconformably overlying the Western Platform carbonates; 4 — Sannio and Molise nappes (Cenozoic upper sequence); 5 — Molise nappe (Mesozoic lower sequence); 6 — Western and Apulia Carbonate Platforms.

documented by 15 geological sections crossing the Apenninic chain with a NE–SW direction from the Tyrrhenian to the Adriatic Sea; four of these sections have been crossed by the seismic refraction line.

In the northern part of the investigated area, the seismic refraction profiles cross the geological sections 9 and 8, respectively, close to shots S2 and S3 (Fig. 9). As for the main structural features, our model is in agreement with the two models proposed by Mostardini and Merlini (1986). The sedimentary successions of the Molise Basin, divided in a Cenozoic upper sequence and Mesozoic lower sequence, are involved in a thrust-and-fold system and tectonically overlay Mesozoic limestones of the Apulia Carbonate Platform. Nevertheless, the geometry in the two models is quite different. In detail, in section 9, the top of the Molise Mesozoic lower sequence is about 1.0 km deeper, and in section 8, the Apulia carbonates are about 0.5 km shallower. We think that our model is more reliable because the 4.8 km/s layer (that has been interpreted as the Molise lower sequence) is constrained both by first-arrival refracted branches from shots S1, S2 and S3 (phases *h4* in Fig. 3a–c) and by reflected arrivals from shots S1 and S2 (phases *r4* in Fig. 3a and b); moreover, subsurface data from S.Croce and Ielsi 2 wells (Fig. 2) and gravity data modelling (Fig. 7a) provide additional constraints on its depth north of shot S2. The deepening of the Apulia Platform between shot points S3 and S4 is well constrained both by ray-tracing modelling of evident time delays and by finite difference waveforms modelling of the first refracted arrivals observed 15–20 km north of shot point S4 (phase *h7* in Figs. 3d and 5c).

In the southern part of the investigated area, the seismic refraction profile crosses the geological sections 7 and 6, respectively, close to shots S4 and S5 (Fig. 9). In geological section 7, a system of thrust sheets formed by Meso-Cenozoic sedimentary rocks of the Lagonegro–Molise Basin tectonically overlies the Apulia Carbonate Platform at a depth of about 5 km (Fig. 9). According to our model, the top of the Apulia carbonates is only 3.1 km deep, and no Mesozoic Lagonegro–Molise Basin sequence occurs. We

think that our interpretation, extremely well constrained by Taurasi well data, is more reliable.

Close to shot S5, the structures displayed in the two models correspond reasonably well, even if the thrust sheet sandwiched between the Western and the Apulia Carbonate Platforms has been interpreted differently. According to Mostardini and Merlini (1986), it corresponds to the Lagonegro–Molise Basin Mesozoic sequence. Conversely, as inferred by the relatively low velocity (4.1 km/s), we prefer to relate it to the Late Tortonian–Upper Messinian sedimentary sequence drilled in the Taurasi well (Fig. 2).

Several 1-D seismic velocity models were proposed to locate earthquakes in the Sannio and Irpinia regions (Bernard and Zollo, 1989; Amato and Selvaggi, 1993; Chiarabba and Amato, 1997) on the basis of the available regional crustal model (Mostardini and Merlini, 1986). From a comparison with our models, we observe velocity values considerably larger at depths ranging from 3–4 km to 10–11 km corresponding to the high-velocity (6.0–6.6 km/s) Apulia Carbonate Multilayer (Fig. 10).

9. Conclusion

This study presents a detailed seismic velocity model of the upper crust beneath the northern sector of the Southern Apennines, inferred from the interpretation of a seismic refraction profile, constrained by well information and commercial seismic lines, and checked by gravity data and by finite difference simulations of the complete seismic wavefield. This model provides new information on the structure of the Southern Apennines thrust belt.

Significant results of this study are as follows:

(1) Sedimentary rocks of basinal domain show P-wave velocities in the 2.8–4.1 km/s range for the Tertiary sequences and 4.8 km/s for the Mesozoic ones. Meso-Cenozoic limestone successions of the Apulia and Western Carbonate Platform present velocities in the 6.0–6.2 km/s range. A striking high seismic velocity (6.6 km/s) characterizes the lower part of the Apulia Carbonate Multilayer, corresponding to the Triassic dolomites and evapo-

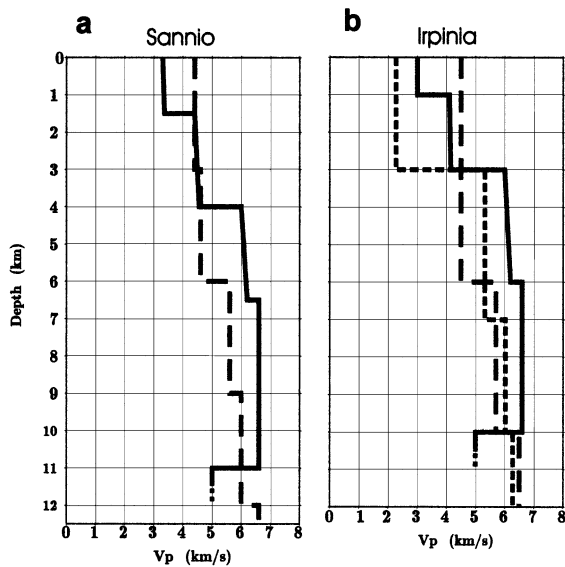


Fig. 10. Comparison with previous 1-D velocity model of the investigated area. (a) Comparison of the 1-D average velocity model of the Sannio region, inferred by this study, (continuous line) with the 1-D velocity model used to localize the background seismicity recorded during 1991–1992 by Chiarabba and Amato (1997) (dashed line); the latter represents the starting model of the 3-D tomographic inversion. (b) 1-D velocity models of the Irpinia region. The continuous line represents the 1-D average velocity model of the north-western sector of Irpinia region inferred by this study. The dotted and dashed lines represent the 1-D velocity models used by Bernard and Zollo (1989) and Amato and Selvaggi (1993), respectively, to calculate the aftershock locations of the 1980 Irpinia earthquake.

rites of the Burano formation. Intermediate–wide-angle reflected arrivals make it possible to define the deepest discontinuity of the model, located at a depth of 9–11 km. The velocity below this interface is unconstrained, but finite difference simulations performed to reproduce the waveforms of the reflected arrivals suggest the presence of a strong inversion of velocity from 6.6 km/s to about 5.0 km/s at the reflecting boundary. This hypothesis is supported by commercial seismic profiles located at the eastern border of the Southern Apennines thrust belt and by two deep wells located in the Apulia foreland that drill Permo-Triassic clastic deposits of the Verrucano formation, characterized by a low seismic velocity (about

5.0 km/s), at the bottom of the Apulia Carbonate Platform.

(2) In the shallower crust (upper 4 km), the velocity model is more homogeneous in the north-western sector than in the southeastern sector (Fig. 4). This can be related to the different structural setting of the Molise–Sannio and Campania–Lucania arcuate segments characterized by a NNW–SSE and WNW–ESE trend of the compressive fronts, respectively (Fig. 1).

(3) Imbricates structures related to the compressional tectonics can explain the thickening (about 6.5 km) of the Apulia Carbonate Platform. Deformation involves mainly evaporites and dolomites of the Burano formation because the anhydrite layers represent highly mobile decollement levels.

(4) The Verrucano formation has been also involved in the thrusts-and-folds system of the Southern Apennines accretionary wedge; thus, the sole thrust of the Southern Apennines belt propagates within the sedimentary Paleozoic strata.

(5) We estimate a minimum thickness of the sedimentary cover in the investigated area of about 9–11 km. This value is in agreement with the isobaths of the magnetic basement (Agip, 1982). Seismic data do not allow us to identify deeper seismic interfaces that could be related to the top of the Paleozoic crystalline basement; this is probably due to the low velocity layer at the bottom of the Carbonate Multilayer that reflects and attenuates a great part of the seismic energy.

(6) Finally, we propose two 1-D average P-wave velocity models of the upper crust both of the Sannio region (Fig. 10) and of the northern part of the Irpinia region (Fig. 10). These models can be used in subsequent studies to localize and interpret past and future seismicity of the Southern Apennines.

Acknowledgements

We thank Dr J. Badal and an anonymous referee for their constructive comments.

References

- Agip, 1982. Aeromagnetic Survey of Italy. A Few Interpretative Results. Agip Internal Report.
- Amato, A., Selvaggi, G., 1993. Aftershock location and P-wave velocity structure in the epicentral region of the 1980 Irpinia earthquake. *Ann. Geofis.* 36, 3–15.
- Amato, A., Montone, P., 1997. Present day stress field and active tectonics in southern peninsular Italy. *Geophys. J. Int.* 130, 519–534.
- Anderson, H.J., Jackson, J., 1987. Active tectonics of the Adriatic region. *J. R. Astron. Soc.* 91, 937–987.
- Bally, A.W., Burbi, L., Cooper, C., Ghelardoni, R., 1986. Balanced sections and seismic reflection profiles across the Central Apennines. *Mem. Soc. Geol. It.* 35, 257–310.
- Bernard, P., Zollo, A., 1989. The Irpinia (Italy) 1990 earthquake: detailed analysis of a complex normal fault. *J. Geophys. Res.* 94, 1631–1648.
- Carrozzo, M.T., Chirenti, A., Luzio, D., Margiotta, C., Quarta, T., 1981. Carta gravimetrica d'Italia: tecniche automatiche per la sua realizzazione. Proc. I Annual Meeting of the National Geophys. Group, Rome, Italy, pp. 132–139.
- Cerveny, V., Molotkov, I.A., Psencik, I., 1977. Ray Method in Seismology. University of Karlova, Prague.
- Chakraborty, K., Agarwal, B.N.P., 1992. Mapping of crustal discontinuities by wavelength filtering of the gravity fields. *Geophys. Prospect.* 40, 801–822.
- Chiarabba, C., Amato, A., 1997. Upper crustal structure of the Benevento area (southern Italy): fault heterogeneities and potential for large earthquakes. *Geophys. J. Int.* 130, 229–239.
- Christensen, N.I., 1982. Seismic velocities. In: Carmichael, R.S. (Ed.), *Handbook of Physical Properties of Rocks*, Vol. 2. CRC Press, Boca Raton, FL, pp. 1–228.
- Corrado, G., Rapolla, A., 1981. The gravity field of Italy: analysis of its spectral composition and delineation of a three dimensional crust model for central-southern Italy. *Boll. Geofis. Teor. App.* 23 (89), 17–29.
- Doglionni, C., Harabaglia, P., Martinelli, G., Mongelli, F., Zito, G., 1996. A geodynamic model of the Southern Apennines accretionary prism. *Terra Nova* 8, 540–547.
- Fedi, M., Rapolla, A., 1990. Aeromagnetic anomaly shape analysis in the Italian region for the evaluation of the crustal block rotations. *J. Geodyn.* 12, 2–4, 149–161.
- Graves, R.W., 1996. Simulating seismic wave propagation in 3D elastic media using staggered-grid finite differences. *Bull. Seismol. Soc. Am.* 86 (4), 1091–1106.
- Iannaccone, G., Improta, L., Biella, G., Castellano, M., Deschamps, A., De Franco, R., Malagnini, L., Mirabile, L., Romeo, R., Zollo, A., 1995. A study of local effects in the Benevento town (Southern Italy) by the analysis of seismic records of explosion. *Ann. Geofis.* 38 (4), 411–427.
- Iannaccone, G., Improta, L., Capuano, P., Zollo, A., Biella, G., De Franco, R., Deschamps, A., Cocco, M., Mirabile, L., Romeo, R., 1998. A P-wave velocity model of the upper crust of Sannio region (Southern Apennines), Italy. *Ann. Geofis.* 41 (4), 567–582.
- Italian Explosion Seismology Group, 1982. Crustal structure in the Southern Apennines region from DSS data reporter S. Scarascia. Proc. EGS–EGC Meeting, Leeds.
- Levander, A.R., 1988. Fourth-order-finite-difference P-SV seismograms. *Geophysics* 53, 1425–1436.
- Malinverno, A., Ryan, W.B.F., 1986. Extension in the Tyrrhenian Sea and shortening in the Apennines as a result of arc migration driven by sinking of the lithosphere. *Tectonics* 5, 227–245.
- Marcellini, A., Iannaccone, G., Romeo, R., Silvestri, F., Bard, P.Y., Improta, L., Meneroud, J.P., Mouroux, P., Mancuso, C., Rippa, F., Simonelli, A., Soddu, P., Tento, A., Vinale, F., 1995a. Benevento seismic risk project: seismotectonic and geotechnical background. Proc. 5th Int. Conf. Seismic Zonation, Nice, France.
- Marcellini, A., Bard, P.Y., Iannaccone, G., Meneroud, J.P., Mouroux, P., Romeo, R., Silvestri, F., Duval, A., Martin, C., Tento, A., 1995b. Benevento seismic risk project: The microzonation. Proc. 5th Int. Conf. Seismic Zonation, Nice, France.
- Marsella, E., Bally, A.W., Cippitelli, G., D'Argenio, B., Pappone, G., 1995. Tectonic history of the Lagonegro domain and Southern Apennines thrust belt evolution. *Tectonophysics* 252, 307–330.
- Marsella, E., Patella, D., Petrillo, Z., Siniscalchi, A., 1998. Magnetotelluric profiles in Southern Apennines. Proc. XXIII Gen. Ass. EGS, 20–24 April 1998, Nice, France.
- Mishra, D.C., Pedersen, L.B., 1982. Statistical analysis of potential fields from subsurface reliefs. *Geoexploration* 19, 247–265.
- Morelli, C., Gantar, T., Honkasalo, T., McConnell, P.K., Tanner, J.B., Szabo, B., Uotila, U., Whalen, C.T., 1974. In: *The International Gravity Standardization Net 1971 (IGSN71)*, IUGG, AIG, Publ. spec. n. 4, Paris, 165–179.
- Mostardini, F., Merlini, S., 1986. Appennino centro-meridionale. *Sezioni geologiche e proposta di modello strutturale*. *Mem. Soc. Geol. It.* 35, 177–202.
- Nafe, J., Drake, C.L., 1963. In: *Physical Properties of Marine Sediments*. The Sea, 3, M.N. Interscience Publ., 74–815.
- Patacca, E., Scandone, P., 1989. Post-Tortonian mountain building in the Apennines. The role of the passive sinking of a relic lithospheric slab. In: Boriani, A., Bonafede, M., Piccardo, G.B., Vai, G.B. (Eds.), *The Lithosphere in Italy*. *Acc. Naz. Lincei* Vol. 80, 157–176.
- Patacca, E., Scandone, P., 1992. The Numidian-sand event in the Southern Apennines. *Mem. Soc. Geol. Padova* 43, 297–337.
- Roure, F., Casero, P., Vially, R., 1991. Growth processes and melange formation in the Southern Apennines accretionary wedge. *Earth Planet. Sci. Lett.* 102, 395–412.
- Spector, A., Grant, F.S., 1970. Statistical models for interpreting aeromagnetic data. *Geophysics* 35, 293–302.
- Talwani, M., Worzel, L., Landisman, M., 1959. Rapid gravity computation for two-dimensional bodies with application to Mendocino submarine fracture zone. *J. Geophys. Res.* 64, 49–59.
- Won, I.L., Bevis, M., 1987. Computing the gravitational and magnetic anomalies due to a polygon. Algorithms and fortan subroutines. *Geophysics* 53, 232–238.